

## Kinetic parameters using an immobilized tetrahexylammonium chloride catalyst in glycidyl methacrylate reaction with carbon dioxide

Sang-Wook Park<sup>†</sup>, Byoung-Sik Choi, Dae-Won Park, Seong-Soo Kim\* and Jae-Wook Lee\*\*

Division of Chemical Engineering, Pusan National University, Busan 609-735, Korea

\*School of Environmental Science, Catholic University, Busan 609-757, Korea

\*\*Department of Chemical Engineering, Sogang University, Seoul 121-742, Korea

(Received 14 December 2006 • accepted 2 April 2007)

**Abstract**—A soluble copolymer-supported catalyst containing pendant tetrahexylammonium chloride was synthesized by the radical copolymerization of *p*-chloromethylated styrene with styrene followed by the addition reaction of the resulting copolymer with trihexylamine. Initial absorption rate of carbon dioxide into glycidyl methacrylate (GMA) solutions containing the catalyst was measured in a semi-batch stirred tank with a plane gas-liquid interface at 101.3 kPa. The reaction rate constants of the elementary reaction between carbon dioxide and GMA were evaluated from analysis of the mass transfer mechanism accompanied by the elementary reactions based on film theory. Solvents such as toluene, *N*-methyl-2-pirrolidinone, and dimethyl sulfoxide influenced the reaction rate constants. Furthermore, this catalyst was compared to monomeric tetrahexylammonium chloride under the same reaction conditions.

Key words: Immobilized Tetrahexylammonium Chloride, Absorption, Carbon Dioxide, Glycidyl Methacrylate

### INTRODUCTION

The chemical fixation of carbon dioxide has received much attention in view of environmental problems. An attractive strategy to deal with this situation is converting CO<sub>2</sub> into valuable substances [1]. The reaction of carbon dioxide with oxiranes leading to 5-membered cyclic carbonates is well known [1]. These cyclic carbonates can be used as polar aprotic solvents, electrolytes for batteries and sources for reactive polymers [2].

The synthesis of cyclic carbonates by the reaction of CO<sub>2</sub> with oxirane has been performed by using Lewis acids, transition metal complexes, and organometallic compounds as catalysts at high pressure such as 10-50 atmospheric pressure [3,4]. Some articles reported the synthesis of 5-membered cyclic carbonates under mild conditions at atmospheric pressure in the presence of metal halides or quaternary onium salts [5-7].

Quaternary onium salts bound to polymer resins have been reported by several authors [6,8,9]. Most published works on resin-bound quaternary onium salts use styrene-divinyl benzene related resins because many technologies are available on these resins due to their use as ion-exchange resin support [10]. Polymer-supported catalysts can be easily separated from reaction mixtures and can be reused.

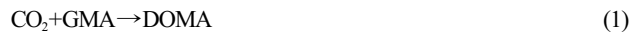
The papers mentioned above about oxirane-CO<sub>2</sub> reactions have focused on the reaction mechanism, the overall reaction kinetics, and the effect of the catalyst on the conversion. But, because the diffusion may have an effect on the reaction kinetics [11] in the mass transfer accompanied by chemical reactions, we believe that it is worthwhile to investigate the effect that diffusion has on the reaction kinetics of the gas-liquid heterogeneous reaction such as the oxirane-CO<sub>2</sub> reaction.

In our previous works, we studied the kinetics in the reaction be-

tween CO<sub>2</sub> and phenyl glycidyl ether using Alquat 336 [12], glycidyl methacrylate (GMA) using 18-crown-6 [13], Alquat 336 [14], and tetrabutylammonium bromide [15] as a catalyst in series. They presented the reaction rate constants as a combined form using the pseudo-first-order reaction method based on the reaction mechanism [4] with two steps. The reaction rate constants of the elemental reactions could not be obtained by the pseudo-first-order reaction method. In this study, the same reaction was performed by using catalysts such as monomeric tetrahexylammonium chloride (THAC) and immobilized tetrahexylammonium chloride. We prepared the immobilized tetrahexylammonium chloride catalyst (we call it as poly-cat.) using a copolymer of styrene and vinylbenzyl chloride, and determined the reaction rate constants and concentration profiles of components in the liquid film using the measured initial absorption rate of CO<sub>2</sub> and the mass transfer mechanism of CO<sub>2</sub> accompanied by chemical reactions. The effect of solvents such as toluene, *N*-methyl-2-pirrolidinone (NMP), and dimethyl sulfoxide (DMSO) on the catalytic activities was observed.

### THEORY

The overall reaction [7] between CO<sub>2</sub> (A) and GMA (B) using a catalyst (QX) at atmospheric pressure to form (2-oxo-1,3-dioxolan-4-yl) methacrylate (DOMA) is proposed as follows:



The overall reaction in Eq. (1) with the rate-determining step of the attack of the anion part of the catalyst to GMA [7] is assumed to consist of two steps [4] as follows:

(i) A reversible reaction between B and QX to form an intermediate complex (C<sub>1</sub>), (ii) An irreversible reaction between A and C<sub>1</sub> to form QX and DOMA(C)



<sup>†</sup>To whom correspondence should be addressed.

E-mail: swpark@pusan.ac.kr



where  $k_1$ ,  $k_2$ , and  $k_3$  are the forward and backward reaction rate constant in reaction (2), and the reaction rate constant in reaction (3), respectively.

The reaction equilibrium constant ( $K_1$ ) in the reversible reaction of Eq. (2) is defined as follows:

$$K_1 = \frac{k_1}{k_2} = \frac{C_{C_{1eq}}}{C_{Beq} C_{QXeq}} \quad (4)$$

It is assumed that species B and QX are nonvolatile and gas phase resistance to absorption is negligible by using pure species A; thus, the concentration of species A at the gas-liquid interface corresponds to equilibrium with the partial pressure of species A in the bulk gas phase.

Under the assumptions mentioned above, the mass balances of species A, B,  $C_1$ , and QX by using the film theory accompanied by chemical reactions and the boundary conditions are given as follows:

$$D_A \frac{d^2 C_A}{dz^2} = k_3 C_1 C_A \quad (5)$$

$$D_B \frac{d^2 C_B}{dz^2} = k_1 C_B C_{QX} - k_2 C_{C1} \quad (6)$$

$$D_{C1} \frac{d^2 C_{C1}}{dz^2} = -k_1 C_B C_{QX} + k_2 C_{C1} + k_3 C_{C1} C_A \quad (7)$$

$$D_{QX} \frac{d^2 C_{QX}}{dz^2} = k_1 C_B C_{QX} - k_2 C_{C1} - k_3 C_{C1} C_A \quad (8)$$

$$z=0; C_A = C_{Ai}; \frac{dC_B}{dz} = 0, \frac{dC_{C1}}{dz} = 0, \frac{dC_{QX}}{dz} = 0 \quad (9)$$

$$z=z_L; C_A = C_{AL}, C_B = C_{BL}, C_{C1} = C_{C1L}, C_{QX} = C_{QXL} \quad (10)$$

The mass balance of QX is

$$Q_o = C_{QX} + C_{C1} \quad (11)$$

Eqs. (5) through Eq. (11) are arranged as dimensionless forms as follows:

$$\frac{d^2 a}{dx^2} = Mac_1 \quad (12)$$

$$\frac{d^2 b}{dx^2} = M\alpha r_B bq - M\beta r_B c_1 \quad (13)$$

$$\frac{d^2 c_1}{dx^2} = -M\alpha r_{C1} c_{BQ} bq + M\gamma r_{C1} c_1 + Mr_{C1} c_{AQ} ac_1 \quad (14)$$

$$x=0; a=1, db/dx=dc_1/dx=0 \quad (15)$$

$$x=1; a=a_L, b=b_L, c_1=c_{1L} \quad (16)$$

$$1=q+c_1 \quad (17)$$

where,  $a = \frac{C_A}{C_{Ai}}$ ,  $b = \frac{C_B}{C_{Bo}}$ ,  $c_1 = \frac{C_{C1}}{Q_o}$ ,  $q = \frac{C_{QX}}{Q_o}$ ,  $M = \frac{k_3 Q_o D_A}{k_L^2}$ ,  $r_B = \frac{D_A}{D_B}$ ,  $r_{C1} = \frac{D_A}{D_{C1}}$ ,  $\alpha = \frac{k_1}{k_3}$ ,  $\beta = \frac{k_1}{K_1 k_3 C_{Bo}}$ ,  $\gamma = \frac{k_1}{K_1 k_3 Q_o}$ ,  $c_{AQ} = \frac{C_{Ai}}{Q_o}$ ,  $c_{BQ} = \frac{C_{Bo}}{Q_o}$ ,  $a_L = \frac{C_{AL}}{C_{Ai}}$ ,  $b_L = \frac{C_{BL}}{C_{Bo}}$ ,  $c_{1L} = \frac{C_{C1L}}{Q_o}$ ,

The enhancement factor (F) of A by chemical reaction is defined

as ratio of the flux of A with reaction and that without reaction based on the film theory as follows:

$$F = \frac{N_A}{N_{A0}} = \frac{-D_A (dC_A/dz)}{k_L (C_{Ai} - C_{AL})} \Big|_{z=0} = -\frac{dz}{dx} \Big|_{x=0} \quad (18)$$

The equilibrium concentration of B ( $C_{Beq}$ ) in the reversible reaction of Eq. (2) is expressed to Eq. (19).

$$C_{Beq} = C_{Bo} (1-x) \quad (19)$$

where, x is the conversion of B, which is obtained as follows:

$$K_1 = \frac{C_{Bo} x}{C_{Bo} (1-x) (Q_o - C_{Bo} x)} \quad (20)$$

The equilibrium concentration of  $C_1$  ( $C_{C1eq}$ ) is expressed from Eq. (4) and (11) as follows:

$$C_{C1eq} = \frac{K_1 C_{Bo} (1-x) Q_o}{1 + K_1 C_{Bo} (1-x)} \quad (21)$$

At the initial time of  $CO_2$  absorption,  $C_B$  and  $C_{C1}$  in the liquid film become to be  $C_{Beq}$  and  $C_{C1eq}$ , respectively, which are constant as shown in Eqs. (19) and (21).

Under the condition of the initial time of  $CO_2$  absorption, Eqs. (5)-(8) become to be one differential equation as follows:

$$D_A \frac{d^2 C_A}{dz^2} = k C_A \quad (22)$$

$$\text{where } k = \frac{k_3 K_1 C_{Bo} (1-x) Q_o}{1 + K_1 C_{Bo} (1-x)} \quad (23)$$

F is derived from the exact solution of Eq. (22) and the definition of F in Eq. (18) as follows:

$$F = \frac{\eta}{\tanh \eta} \quad (24)$$

$$\text{where, } \eta = \sqrt{k_3 K_1 D_A C_{Bo} Q_o / (1 + K_1 C_{Bo})} / k_L \quad (25)$$

Eq. (25) is rearranged as follows:

$$\frac{Q_o}{(\eta k_L)^2} = \frac{1}{k_3 D_A} + \frac{1}{k_3 D_A K_1 C_{Bo}} \quad (26)$$

The values of  $k_3$  and  $K_1$  are obtained from the plots of left side of Eq. (26) vs.  $1/C_{Bo}$ , where  $\eta$  comes from Eq. (24) by using the measured F.

$C_{AL}$ ,  $C_{BL}$ , and  $C_{C1L}$  of the boundary condition of Eq. (10), which are needed to solve Eqs. (5)-(8), are obtained as follows:

At the initial time,  $C_{BL}$  and  $C_{C1L}$  become to be  $C_{Beq}$  and  $C_{C1eq}$  in Eqs. (19) and (21). If the diffusion rate of A is not smaller than the reaction rate and the amount of the dissolved A that reacts in the diffusion film adjacent to the phase boundary compared to that which reaches the bulk liquid phase in the unreacted state is negligible, the concentration of A in the bulk phase ( $C_{AL}$ ) is a finite quantity [11].  $C_{AL}$  can be obtained from the following equation:

$$k_L a (C_{Ai} - C_{AL}) = k_3 C_{C1eq} C_{AL} \quad (27)$$

## EXPERIMENTAL

### 1. Chemicals

**Table 1. Physical properties of CO<sub>2</sub>/GMA/poly-cat and THAC system**

Temp. (°C)	Solvent	$\mu$ (cp)	$C_{Ai}$ (kmol/m <sup>3</sup> )	$D_A \times 10^9$ (m <sup>2</sup> /s)	$D_B \times 10^9$ (m <sup>2</sup> /s)	$D_{C1} \times 10^9$ (m <sup>2</sup> /s)	$k_{Lo} \times 10^5$ (m/s)
80	Toluene	0.362(0.322)	0.0783	8.683(9.379)	3.393(3.665)	1.977(2.136)	2.893(3.125)
	NMP	0.875(0.848)	0.0711	3.618(3.694)	1.414(1.444)	0.892(0.890)	1.7981.836)
	DMSO	0.986(0.857)	0.0612	2.955(3.245)	1.155(1.268)	0.662(0.727)	1.340(1.472)
85	Toluene	0.351(0.307)	0.0727	9.133(9.977)	3.568(3.898)	2.054(2.246)	3.310(3.616)
	NMP	0.831(0.797)	0.0679	3.877(3.986)	1.515(1.558)	0.928(0.954)	1.861(1.914)
	DMSO	0.950(0.808)	0.0576	3.132(3.490)	1.224(1.364)	0.692(0.771)	1.702(1.897)
90	Toluene	0.334(0.294)	0.0698	9.704(10.56)	3.792(4.128)	2.192(2.387)	3.692(4.019)
	NMP	0.772(0.750)	0.0629	4.2134.295)	1.646(1.678)	1.016(1.036)	2.307(2.352)
	DMSO	0.863(0.764)	0.0544	3.452(3.743)	1.349(1.463)	0.783(0.849)	2.025(2.196)

Numbers in parentheses are the physical properties for THAC.

All chemicals were of reagent grade and were used without further purification. Purity of both CO<sub>2</sub> and N<sub>2</sub> was more than 99.9%. GMA, styrene (ST), vinylbenzyl chloride (VBC), and 2,2'-azobisisobutyronitrile (AIBN) were supplied by Aldrich chemical company, U.S.A.

## 2. Absorption Procedure

A semi-batch stirred tank (0.075 m inside diameter, 0.13 m height, agitation speed of 50 rpm) with a plane gas-liquid interface was used to measure the outlet flow rate of CO<sub>2</sub> by using a mass flow meter (Brook Instrument, U.S.A) in GMA solutions in the range of 0.5-3 kmol/m<sup>3</sup> with catalyst at temperature in the range of 80-90 °C. The concentration of CO<sub>2</sub> in the bulk body of the liquid (C<sub>AL</sub>) at a given absorption time was obtained from the difference of the inlet and outlet flow rate of gas of the absorber [16]. The flow rate of CO<sub>2</sub> at the inlet was maintained at 50 cm<sup>3</sup>/min. The experimental procedure used to obtain the absorption rate of CO<sub>2</sub> was identical to that described earlier [15].

## 3. Preparation of Catalyst

Copolymer of ST and VBC was synthesized by the radical copolymerization of VBC (31.3 mole%) with ST (68.7 mole%) with AIBN as an initiator in toluene at 60 °C for 5 hours, and then at 80 °C for 2 h under nitrogen gas, followed by precipitation into methanol and two reprecipitations from tetrahydrofuran (THF) solution into methanol. The VBC unit in the synthesized copolymer was measured by <sup>1</sup>H-NMR and its value was 41 mole%. The copolymer was reacted with trihexylamine in dimethylformamide (DMF) at 80 °C for 48 hours. The resulting polymer was purified by reprecipitating twice from methanol solution into diethyl ether, and dried at 50 °C under vacuum to obtain the catalyst. The attached amount of N<sup>+</sup> in the catalyst was measured by the elemental analysis and its value was 1.46 mmol/g-catalyst, and the VBC unit with N<sup>+</sup> in the catalyst was calculated and its value was 26 mole%. The preparation procedure to obtain the soluble polymer-supported catalyst containing pendant tetrahexylammonium chloride residue was reported elsewhere [17].

## 4. Physical Properties of CO<sub>2</sub> and GMA

The solubility (C<sub>AI</sub>) of CO<sub>2</sub> in organic solvents such as toluene, NMP, and DMSO at 101.3 kPa was obtained by measuring the pressure difference of CO<sub>2</sub> before and after equilibrium between gas and liquid phase, similar to the procedure reported elsewhere [18]. Diffusivity (D<sub>A</sub>, D<sub>B</sub>, D<sub>C1</sub>) of CO<sub>2</sub>, GMA, and C<sub>1</sub> in solvent was estimated from the Wilke-Chang equation [19]. The solvent viscosity

( $\mu$ ) was measured with a Cannon-Fenske viscometer. The viscosity of solvent, solubility, mass transfer coefficient, diffusivities of CO<sub>2</sub>, GMA, and C<sub>1</sub> in each solvent are listed in Table 1. Numbers in parentheses are those for THAC.

## 5. Analysis of DOMA

The presence of DOMA, which was produced from the reaction between CO<sub>2</sub> and GMA using poly-cat and THAC, respectively, was confirmed to be same by instrumental analysis, such as FT-IR (cyclic carbonate C=O peak at 1,800 cm<sup>-1</sup>) and <sup>13</sup>C-NMR (cyclic carbonate C=O at 160 ppm) spectra, which were same as those measured in previous studies [15].

## RESULTS AND DISCUSSION

The procedure employed to determine k<sub>L</sub> is based on measuring the amount of gas absorbed, according to:

$$\frac{dC_{AL}}{dt} = k_L a_V (C_{AI} - C_{AL}) \quad (28)$$

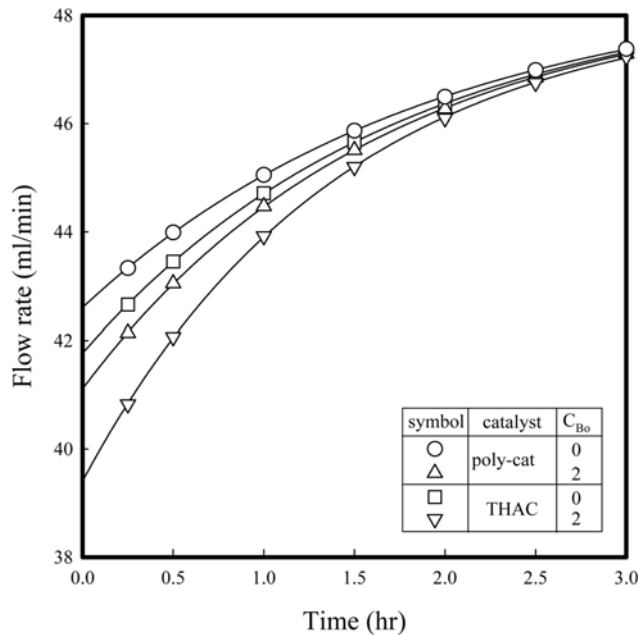


**Fig. 1. Flow rate of gas at outlet vs. time in DMSO solution of GMA at  $Q_o = 0.01$  kmol/m<sup>3</sup> and 85 °C.**

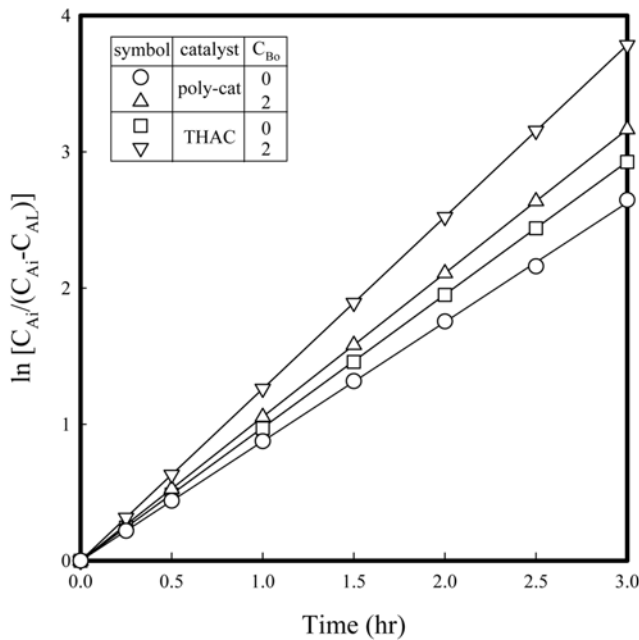


Fig. 2.  $\ln[C_{Ai}/(C_{Ai} - C_{AL})]$  vs. time under the same condition listed in Fig. 1.

where  $a_v$  is the specific contact area at the gas-liquid interface, and its value was  $14.287 \text{ m}^2/\text{m}^3$ .

Integrating Eq. (28), the graphical representation of  $\ln[C_{Ai}/(C_{Ai} - C_{AL})]$  vs. time is obtained from the following equation:

$$\ln[C_{Ai}/(C_{Ai} - C_{AL})] = k_L a_v t \quad (29)$$

Fig. 1 shows typical plots of the measured flow rate of gas at the outlet against the absorption time in DMSO solution of GMA containing poly-cat and THAC of  $0.01 \text{ kmol/m}^3$ , respectively, at  $85^\circ\text{C}$ . As shown in Fig. 1, the measured flow rate increases with increasing the absorption time, and decreases with increasing the GMA concentration. Also, the flow rate for poly-cat is larger than that for THAC.

Fig. 2 is a typical plot of  $\ln[C_{Ai}/(C_{Ai} - C_{AL})]$  vs. time under the same experimental conditions as those listed in Fig. 1. The plots in Fig. 2 show straight lines through the origin, from the slope of which the  $k_L$  were obtained. The mass transfer coefficients without a chemical reaction ( $k_{Lo}$ ) are listed in Table 1.

Generally, the experimental F due to the chemical reaction in gas absorption is obtained as a ratio of the absorption rate with reaction to that without reaction in a continuous absorber, or the ratio of the liquid-side mass transfer coefficient ( $k_L$ ) of gas with reaction to that ( $k_{Lo}$ ) without reaction [20] (20) in a semi-batch absorber. F in this

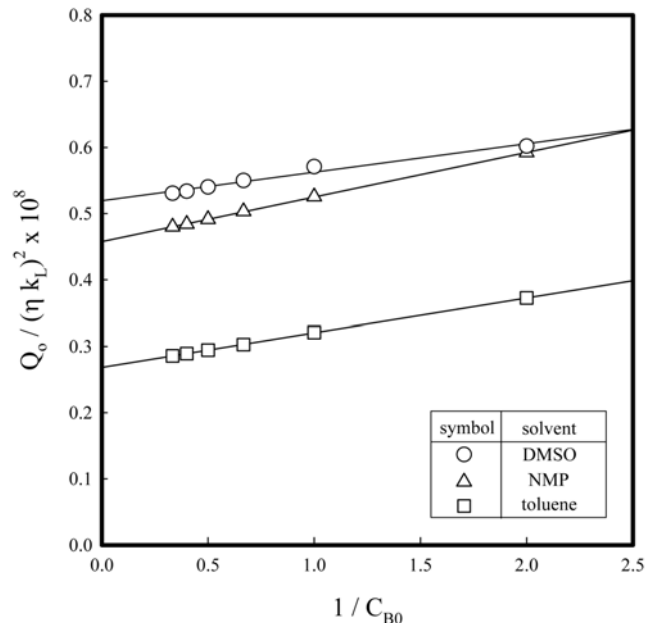


Fig. 3.  $Q_o / (\eta k_L)^2 \times 10^8$  vs.  $1/C_{Bo}$  for various solvents.

study was obtained from the ratio of  $k_L$  to  $k_{Lo}$ . And then, the value of  $\eta$  was obtained from Eq. (24) by using the experimental F.

Fig. 3 shows plots of  $Q_o / (\eta k_L)^2$  against  $1/C_{Bo}$  for various solvents with poly-cat of  $0.01 \text{ kmol/m}^3$  at  $85^\circ\text{C}$ ; these plots satisfy straight lines. The values of  $k_3$  and  $K_1$  were obtained from the intercept and slope of these straight lines. The values of  $k_3$  and  $K_1$  in toluene, NMP and DMSO at  $85^\circ\text{C}$  were  $2.363 \text{ m}^3/\text{kmol}\cdot\text{s}$ ,  $2.24 \text{ m}^3/\text{kmol}$ ,  $3.59 \text{ m}^3/\text{kmol}\cdot\text{s}$ ,  $4.547 \text{ m}^3/\text{kmol}$ ,  $4.557 \text{ m}^3/\text{kmol}\cdot\text{s}$  and  $6.546 \text{ m}^3/\text{kmol}$ , respectively, which are listed in Table 2.

As shown in the differential equations of Eqs. (12)-(14) and the boundary conditions of Eqs. (15)-(17), the physico-chemical properties are required to solve the differential equations and to obtain the theoretical F at the given  $C_{Bo}$  and  $Q_o$ . Every value of the physico-chemical properties except  $k_1$  is given in Table 1 and 2. The value of  $k_1$  is adjusted by trial and error to obtain the minimum deviation between F calculated from Eq. (18) and the experimental F. The values of F are calculated according to the change of  $k_1$  from the solution of Eqs. (12)-(14) and Eq. (18). The plots of calculated F vs.  $k_1$  are shown in Fig. 4 under the typical condition of  $C_{Bo}=3 \text{ kmol/m}^3$ ,  $Q_o=0.01 \text{ kmol/m}^3$  in DMSO at  $85^\circ\text{C}$ . Although F changes little for large change of  $k_1$  and it may not be easy to find an accurate value of  $k_1$  as shown in Fig. 4, the value of  $k_1$  may be adjusted as  $80 \text{ m}^3/\text{kmol}\cdot\text{s}$  in this typical condition, because F of 1.2079 approaches the experimental F of 1.2080 at  $80 \text{ m}^3/\text{kmol}\cdot\text{s}$  of  $k_1$ .

Table 2.  $K_1$  and  $k_3$  of  $\text{CO}_2/\text{GMA}/\text{poly-cat}$  and THAC system

Temp. ( $^\circ\text{C}$ )	80		85		90		
	Rate constant	$K_1$ ( $\text{m}^3/\text{kmol}$ )	$k_3$ ( $\text{m}^3/\text{kmol}\cdot\text{s}$ )	$K_1$ ( $\text{m}^3/\text{kmol}$ )	$k_3$ ( $\text{m}^3/\text{kmol}\cdot\text{s}$ )	$K_1$ ( $\text{m}^3/\text{kmol}$ )	$k_3$ ( $\text{m}^3/\text{kmol}\cdot\text{s}$ )
Toluene		2.55(4.08)	2.51(4.63)	5.16(5.96)	4.08(6.14)	5.35(8.11)	6.13(8.83)
NMP		4.18(6.24)	3.34(6.99)	6.79(8.24)	5.64(9.05)	10.58(12.55)	8.81(11.52)
DMSO		5.81(7.82)	3.89(8.69)	8.50(9.87)	6.26(10.11)	11.64(14.86)	9.56(14.28)

Numbers in parentheses are the reaction rate constants for THAC.

The concentrations of  $\text{CO}_2$ , GMA,  $\text{C}_1$ , and QX in the liquid film are obtained from the numerical solution of Eqs. (12)-(14) using the finite element method with the dimensionless parameters containing the adjusted  $k_i$ . At the typical condition of  $\text{C}_{\text{Bo}}=0.5 \text{ kmol/m}^3$ ,  $\text{Q}_0=0.01 \text{ kmol/m}^3$  in DMSO at 85 °C, the dimensionless concentration profiles of  $\text{CO}_2$ , GMA,  $\text{C}_1$ , and QX in the liquid film are

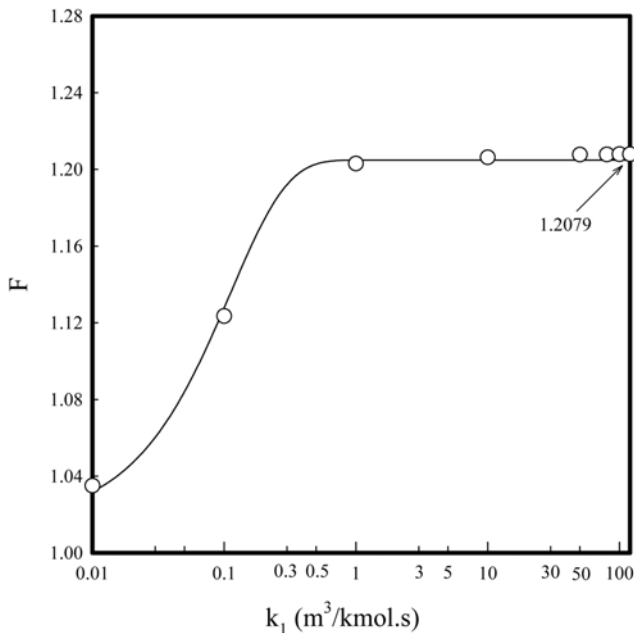


Fig. 4.  $F$  vs.  $k_i$  at  $\text{C}_{\text{Bo}}=3 \text{ kmol/m}^3$  in DMSO solution at 85 °C.

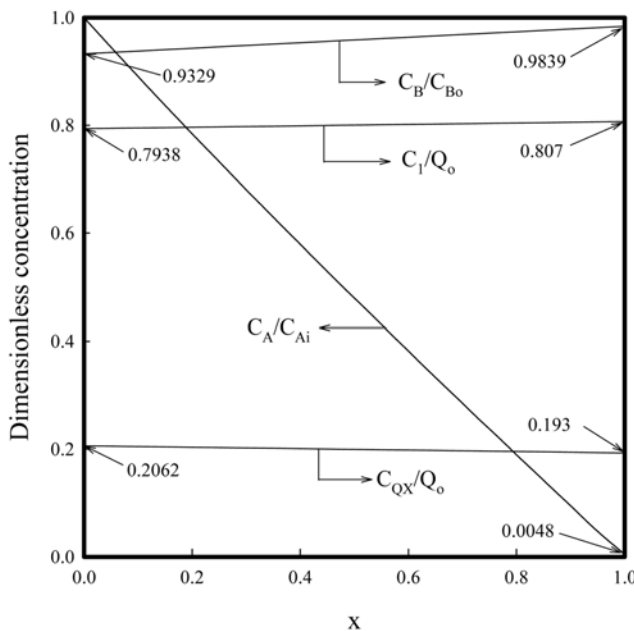


Fig. 5. Dimensionless concentration profile of  $\text{CO}_2$ , GMA,  $\text{C}_1$  and QX in the liquid film under the condition such as  $\text{C}_{\text{Bo}}=0.5 \text{ kmol/m}^3$ ,  $\text{Q}_0=0.01 \text{ kmol/m}^3$ , DMSO, and 85 °C. Dimensionless parameters:  $M=0.6765$ ,  $\alpha=15.98$ ,  $\beta=3.761$ ,  $\gamma=188.023$ ,  $r_B=2.5588$ ,  $r_{\text{Cl}}=4.5272$ ,  $c_{\text{AQ}}=5.76$ ,  $c_{\text{BQ}}=50$ ,  $a_L=0.0049$ ,  $b_L=0.9839$ ,  $c_{\text{L}}=0.807$ .

illustrated in Fig. 5. The dimensionless parameters at the typical condition are listed in Fig. 5. As shown in Fig. 5,  $C_A$  and  $C_{\text{QX}}$  decrease, and  $C_B$  and  $C_{\text{Cl}}$  increase with increasing the depth of the liquid film ( $x$ ).

To observe the effect of  $F$  on the concentration of GMA, the initial absorption rates of  $\text{CO}_2$  were measured according to changes of the GMA concentration over the range of 0.5-3  $\text{kmol/m}^3$  in each solvent. The plots of the experimental values of  $F$  against  $\text{C}_{\text{Bo}}$  are typically shown as open marks in Fig. 6. The solid line in Fig. 6 pres-

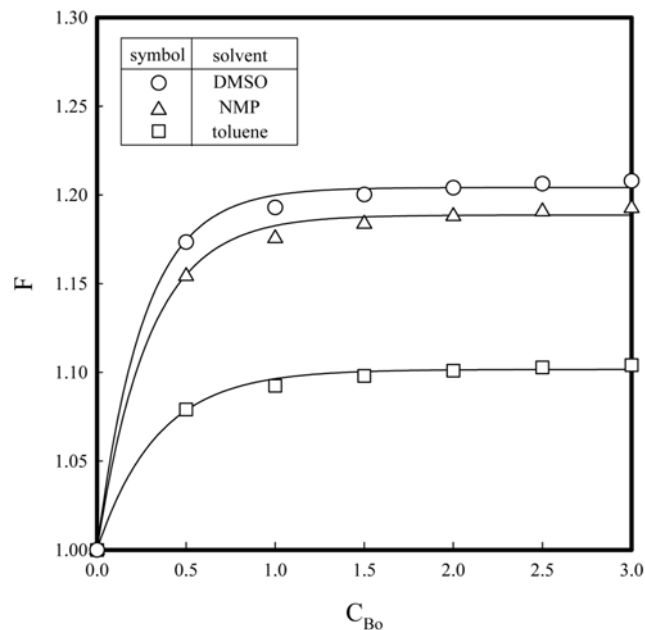


Fig. 6.  $F$  vs.  $\text{C}_{\text{Bo}}$  for various solvents with poly-cat of  $0.01 \text{ kmol/m}^3$  at 85 °C.

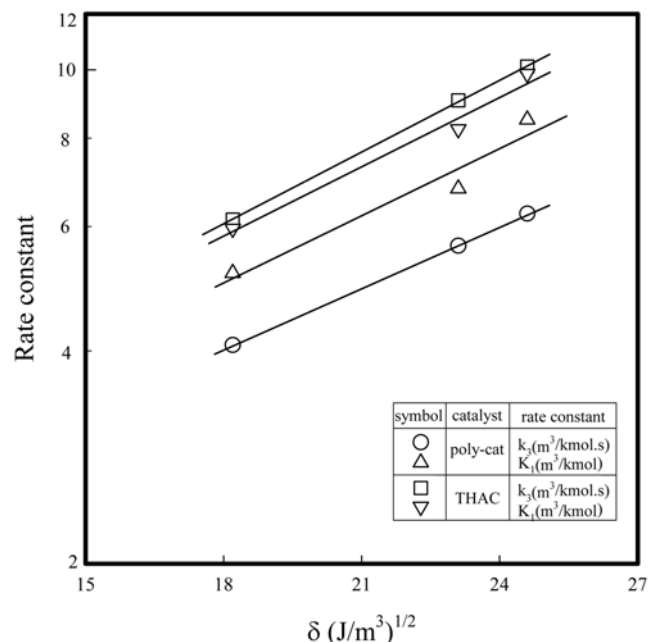


Fig. 7. Relationship between reaction rate constant and solubility parameter of solvent.

ents the calculated  $F$ , which is obtained by using the procedure mentioned above. As shown in Fig. 6,  $F$  increases with increasing GMA concentration and increases in the order toluene, NMP, DMSO.

The rate reaction constants in an organic reaction in a solvent generally reflect the solvent effect. Various empirical measurements about the solvent effect have been proposed to correlate with the reaction rate constant [21]. Some of them have a linear relationship to solubility parameter ( $\delta$ ) of solvent. Then, to observe  $\delta$  on the reaction rate constant, the initial absorption rates of  $\text{CO}_2$  were measured in solution of toluene, NMP and DMSO, respectively. Table 2 presents the values of  $k_3$  and  $K_1$  for various solvents and those for THAC as numbers in parenthesis. Fig. 7 shows typical plots of logarithms of  $k_3$  and  $K_1$  vs.  $\delta$  with poly-cat and THAC by using  $\delta$  [22] of toluene, NMP and DMSO of 18.2, 23.1, and 24.6 ( $\text{J}/\text{m}^{0.5}$ ), respectively; the plots satisfy the linear relationship between the reaction rate constant and  $\delta$ . The solvent polarity is increased with increasing  $\delta$ . It may be assumed that increased instability and solvation of  $\text{C}_1$  arising from the increased solvent polarity enhance the dissociation reaction of  $\text{C}_1$  and the reaction between  $\text{C}_1$  and  $\text{CO}_2$ , such as  $\text{SN}_1$  (nucleophilic substitution) by solvation [23], respectively; thus, the values of  $K_1$  and  $k_3$  increase upon increasing  $\delta$ , as shown in Fig. 7. This result coincides with that of Nishikubo et al. [9]. They presented that the yield of cyclic carbonate increased in the order toluene, NMP, DMSO in the addition reaction of 2-phenoxy-methyloxirane with  $\text{CO}_2$  using soluble polymer-supported catalyst with quaternary onium salt and explained the increase of the product with aprotic polarity.

To observe the effect of reaction temperature on the reaction rate constants, absorption rates of  $\text{CO}_2$  were measured according to changes of the reaction temperature over the range of 80–90 °C. Table 2 presents the values of  $k_3$  and  $K_1$  for various temperatures. Fig. 8 shows typical plots of  $k_3$  and  $K_1$  against  $1/T$  in a semi-logarithm scale in DMSO solution; the plots satisfy straight lines. The activation energy

of reaction (3) was obtained from the slope of the plots for  $k_3$ ; its value is 22.9 kcal/mol.

To compare the catalytic activity of poly-cat with that of the corresponding monomeric quaternary onium salt,  $k_3$  and  $K_1$  for THAC of 0.01 kmol/m<sup>3</sup> were obtained by the same procedure as that for poly-cat and shown as numbers in parentheses, and they are plotted vs.  $\delta$  and  $1/T$  in Figs. 7 and 8, respectively. As shown in Figs. 7 and 8,  $K_1$  and  $k_3$  for poly-cat are smaller than those for THAC and the activation energy of reaction (3) for THAC is 12.6 kcal/mol. It is generally known that immobilized quaternary salt catalysts have lower catalytic activity than homogeneous ones [9] as shown in this study. However, a distinct comparison of the reactivity of homogeneous and immobilized quaternary salt catalysts is not easy since the structure of cation and counter anion of the catalyst greatly affects the catalytic performance.

## CONCLUSIONS

The overall reaction between  $\text{CO}_2$  and GMA with immobilized THAC as a catalyst was assumed to consist of two elementary reactions: the reversible reaction of GMA and the catalyst to form an intermediate, and an irreversible reaction of this intermediate with carbon dioxide to form five-membered cyclic carbonate. Initial absorption rate of  $\text{CO}_2$  was used to obtain the reaction rate constant of the elementary reaction and the concentration profile of each component in the liquid film from the numerical solution of the diffusion equations accompanied by the elementary reactions. The solubility parameter of solvent influenced the reaction rate constants.

## ACKNOWLEDGMENTS

This work was supported from the Basic Research Program of the Korea Science and Engineering Foundation (KOSEF) through the Applied Rheology Center (ARC) and Brain Korea 21 Project.

## REFERENCES

1. M. Aresta, *Carbon dioxide recovery and utilization*, Kluwer Academic Publishers, London (2003).
2. K. Weissermel and H. Arpe, *Industrial organic chemistry*, Wiley-VCH, Weinheim, New York (1997).
3. W. J. Peppel, *Ind. Eng. Chem.*, **50**, 767 (1958).
4. G. Rokicki, *Makromol. Chem.*, **186**, 331 (1985).
5. T. Aida and S. Inoue, *J. Am. Chem. Soc.*, **105**, 1304 (1983).
6. Y. Nishikubo, T. Kato, S. Sugimoto, M. Tomoi and S. Ishigaki, *Macromolecules*, **23**, 3406 (1990).
7. N. Kihara and T. Endo, *Macromolecules*, **25**, 4824 (1992).
8. T. Nishikubo, A. Kameyama, J. Yamashida, M. Tomoi and W. Fukuda, *J. Polym. Sci., Part A: Polym. Chem.*, **31**, 939 (1993).
9. T. Nishikubo, A. Kameyama, J. Yamashida, T. Hukumitsu, C. Maejima and M. Tomoi, *J. Polym. Sci., Part A: Polym. Chem.*, **33**, 1011 (1995).
10. C. M. Starks, C. L. Liotta and M. Halpern, *Phase transfer catalysis*, Chapman & Hall, New York (1984).
11. L. K. Daraivswany and M. M. Sharma, *Heterogeneous reaction: analysis, example and reactor design*, John Wiley & Sons, New York (1980).

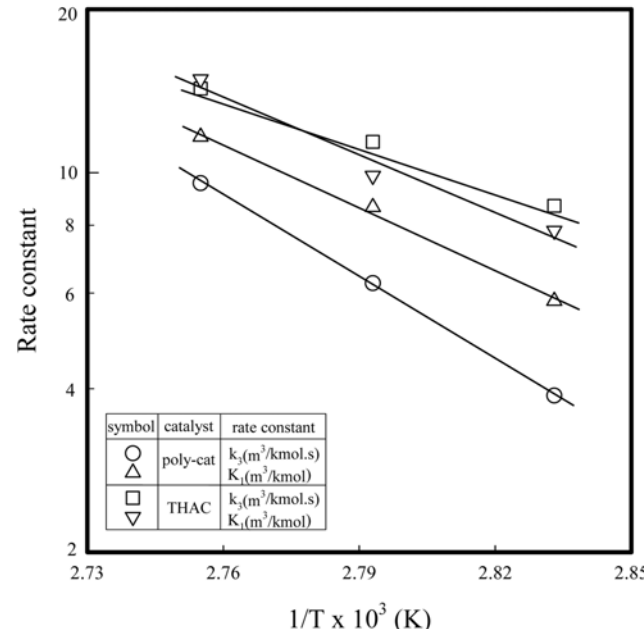


Fig. 8. Dependence of reaction temperature on reaction rate constant in DMSO solution

12. S. W. Park, D. W. Park, T. Y. Kim, M. Y. Park and K. J. Oh, *Catal. Today*, **98**, 493 (2004).
13. S. W. Park, B. S. Choi, D. W. Park and J. W. Lee, *J. Ind. Eng. Chem.*, **11**, 527 (2005).
14. S. W. Park and J. W. Lee, *Stud. Surface Sci. Catal.*, **159**, 345 (2006a).
15. S. W. Park, B. S. Choi, B. D. Lee, D. W. Park and S. S. Kim, *Sep. Sci., Technol.*, **41**, 829 (2006b).
16. D. Gomez-Diaz, J. C. Mejuto and J. M. Navaza, *Chem. Eng. Sci.*, **61**, 2330 (2006).
17. B. S. Yu, E. S. Jeong, K. H. Kim, D. W. Park, S. W. Park and J. W. Lee, *React. Kinet. Catal. Lett.*, **84**, 175 (2005).
18. M. L. Kennard and A. Meisen, *J. Chem. Eng. Data*, **29**, 309 (1984).
19. P. V. Danckwerts, *Gas-liquid reaction*, McGraw-Hill Book Company, New York (1970).
20. S. W. Park, K. W. Kim and I. J. Sohn, *Sep. Purif. Technol.*, **19**, 43 (2000).
21. H. F. Herbrandson and F. B. Neufeld, *J. Org. Chem.*, **31**, 1140 (1996).
22. J. Brandrup and E. H. Immergut, *Polymer handbook*, Second Ed., John Wiley & Sons, New York (1975).
23. R. T. Morrison and R. N. Boyd, *Organic chemistry*, Fourth Ed, Allyn and Bacon, Inc, Toronto (1983).